# Identification of the Critical Residues Involved in Peptidoglycan Detection by Nod1

Stephen E. Girardin, Muguette Jéhanno, Dominique Mengin-Lecreulx,
Philippe Sansonetti, Pedro M. Alzari, Dana J. Philpott

# Identification of the Critical Residues Involved in Peptidoglycan Detection by Nod1*[S]

**Stephen E. Girardin**[‡§1,2], **Muguette Jéhanno**[¶1], **Dominique Mengin-Lecreulx**[‖], **Philippe J. Sansonetti**[‡],
**Pedro M. Alzari**[**], and **Dana J. Philpott**[¶1]

*From the* ‡*Unité de Pathogénie Microbienne Moléculaire, INSERM U389,* §*Groupe Inserm Avenir "Peptidoglycan and Innate Immunity,"* ¶*Groupe Immunité Innée et Signalisation,* **\*\**Unité de Biochimie Structurale, Institut Pasteur, 28 Rue du Dr. Roux, 75724 Paris Cedex 15, France and the* ‖*Enveloppes Bactériennes et Antibiotiques, IBBMC, UMR 8619 CNRS, Université Paris-Sud, Bât. 430, 91405 Orsay, France*

**Nod1 is an intracellular pattern recognition molecule activated following bacterial infection, which senses a specific muropeptide (L-Ala-D-Glu-*meso*-DAP (diaminopimelic acid); "Tri$_{DAP}$") from peptidoglycan. Here we investigated the molecular basis of Tri$_{DAP}$ sensing by human (h) Nod1. Our results identified the domain responsible for Tri$_{DAP}$ detection in the center of the concave surface of hNod1 leucine-rich repeat domain. Amino acid residues critical for sensing define a contiguous surface patch that is largely conserved in Nod1 proteins from different species. Accordingly, the distinct specificities of human *versus* murine Nod1 toward muropeptide detection were also found to lie in this central cleft. Several splicing variants of Nod1 lacking repeats 7–9 have been characterized recently, the relative balance of which is thought to correlate with the onset of asthma or inflammatory bowel disease. We demonstrated that these isoforms failed to transduce NF-κB activation upon muropeptide stimulation. This study provided insights into the molecular mechanisms responsible for the detection of bacterial peptidoglycan by Nod1 and suggested that defects in Nod1-dependent peptidoglycan sensing may contribute to elicit certain inflammatory disorders.**

The innate immune system has evolved means to mediate recognition of microbes through the specific detection of highly conserved structures. Such conserved microbial motifs are generally molecules from the cell wall or nucleic acids, and in the case of bacteria, these include lipopolysaccharide, peptidoglycan, lipoproteins, lipoteichoic acid, flagellin, and CpG DNA. Recently, studies focusing on the innate immune responses to peptidoglycan have gained substantial attention through the identification of new classes of peptidoglycan sensors, both in mammals and *Drosophila* (1). Peptidoglycan recognition proteins (PGRPs)[3] exist in vertebrates and arthropods, and their ability to bind to

peptidoglycan appears to represent a common property (2). However, although a clear role for PGRPs in triggering innate immune responses has been demonstrated unequivocally in *Drosophila*, the function of mammalian PGRPs remains elusive. In addition to PGRPs, recent evidence has now clearly identified the Nod proteins, Nod1 and Nod2, which are two members of the growing family of Nod-like receptors (NLRs; also known as CATERPILLER), as intracellular sensors of peptidoglycan (3–5). Within the peptidoglycan polymer, Nod1 and Nod2 detect highly specific substructures, MurNAc-L-Ala-D-Glu-*meso*-DAP (M-Tri$_{DAP}$) and MurNAc-L-Ala-D-Glu (muramyl dipeptide or MDP), respectively (6–10).

Upon activation, Nod proteins trigger the activation of NF-κB, c-Jun N-terminal kinase/stress-activated protein kinase, and caspase pathways, which in turn governs some of the host responses to bacterial infection. Nod proteins have been shown to play a key role in host response to a variety of bacterial infections, including *Shigella flexneri*, enteroinvasive *Escherichia coli*, *Helicobacter pylori*, *Listeria monocytogenes*, *Chlamydophila pneumoniae*, *Streptococcus pneumoniae*, and *Pseudomonas aeruginosa* (11–17). In addition, the key role of Nod proteins in the modulation of inflammatory processes is highlighted by the recent identification of the genetic association between mutations in *Nod2* and several inflammatory disorders, including Crohn's disease (18, 19), Blau syndrome (20), and early onset sarcoidosis (21). More recently, studies have also identified polymorphisms in *Nod1* associated with genetic predisposition to inflammatory bowel disease (22), atopic eczema (23), and asthma (24). However, in the latter case, a link between the genetic observation and any functional significance remains to be clearly addressed, because the polymorphisms found lie within the ninth intron of the *Nod1* gene. It has been proposed by the authors of the two studies that these mutations might affect the relative abundance of specific Nod1 splice variants.

It is becoming clear that Nod proteins, via the specific detection of muropeptide motifs, are key molecules involved in innate immunity and inflammation. However, the molecular basis of peptidoglycan detection by Nods remains largely undefined. First, it is still not known whether Nod proteins interact directly with peptidoglycan fragments or whether sensing involves additional protein intermediates. Also, crystal structures of Nod LRR domains are still lacking, which restricts our current knowledge of structure-function for these pattern-recognition molecules (PRMs). In the case of Toll-like receptors (TLRs), the most widely studied family of mammalian pattern-recognition molecules, detection of microbial patterns also occurs through the LRR ectodomain. Still, a decade of intensive investigation on TLRs did not lead to substantial understanding of microbial detection by TLRs at a molecular level. However, with the recent characterization of the first structure of the

LRR domain from TLR3 (25), one can now expect that some of these questions will be solved in the near future.

In this context, we have undertaken an approach based on mutagenesis (either deletions or site-directed point mutations) to gain more insight into the molecular basis of peptidoglycan detection by Nod1. We mapped the region responsible for $Tri_{DAP}$ sensing within Nod1 LRR to a contiguous patch of amino acid residues in the center of the inner concave surface of the LRR. Because recent evidence has identified the existence of several Nod1 splicing variants and their correlation with an increased risk for asthma and inflammatory bowel disease (22, 24), we analyzed these variants for their ability to sense peptidoglycan and muropeptides. These isoforms all contained only a part of the $Tri_{DAP}$ sensing domain, and consequently, we observed that only the full-length molecule could transduce NF-$\kappa$B activation upon stimulation. Together, this study illustrates the importance of defining with precision the molecular determinants responsible for detection of peptidoglycan by Nod1 and suggests a link between defective Nod signaling and the onset of inflammatory disorders.

## MATERIALS AND METHODS

*Muramyl Peptides*—The experimental procedures relative to the synthesis of the muramyl peptides used in this study have been described elsewhere (8).

*Reagents*—Endotoxin-free fetal calf serum was from Hyclone (Logan, UT) and was used after heat inactivation 56 °C for 30 min. All cell culture reagents and antibiotics were from Invitrogen.

Muramyl dipeptide (MDP-LD) was from Calbiochem and reported to be 98% pure by TLC. Synthetic FK156 was obtained from Fujisawa Inc. (Japan).

*Limulus Amebocyte Assay*—All reagents used in this study tested negative for lipopolysaccharide contamination by the *Limulus* amebocyte assay, according to manufacturer's recommendations (QCL-1000, BioWhittaker, Verviers, Belgium). These reagents include M-Tri$_{DAP}$, Tri$_{DAP}$, MDP, and FK156.

*Expression Plasmids and Transient Transfections*—The expression plasmid for human Nod1 was from Gabriel Nunez (Ann Arbor, MI). The expression plasmid for human Nod2 was from Gilles Thomas (Fondation Jean Dausset/CEPH, Paris, France). The expression plasmid for mouse Nod1 was from InvivoGen (Toulouse, France). The chimeric molecules hNod1-LRR hNod2 and hNod1-LRR hIPAF were obtained by PCR, using standard procedures. The expression plasmid for human IPAF was from Jurg Tschopp and Fabio Martinon (ISREC, Lausanne, Switzerland). The site chosen for the domain swap in hNod1 sequence was amino acid 641 (VESF ↓ NQV). On the side of hNod2 and hIPAF sequences, the sites chosen for swapping were positions 730 (APGE ↓ AKSV) and 595 (IPDY ↓ LFDF), respectively. The empty vector pcDNA3.1 and the NF-$\kappa$B reporter Ig$\kappa$-luciferase were from Invitrogen. Transfections were carried out using FuGENE (Roche Applied Science) in HEK293 as described previously (10).

*NF-$\kappa$B Activation Assays*—Human embryonic kidney HEK293T cells were cultured in Dulbecco's modified Eagle's medium supplemented with 10% fetal calf serum. Studies on the synergistic activation of NF-$\kappa$B by peptidoglycans or muramyl peptides were carried out as described previously (10, 26). Briefly, cells were transfected with 75 ng of the reporter plasmid Ig$\kappa$-luc plus the following vectors: 1 ng of hNod1 or hNod2, 0.5 ng of mNod1. Muramyl peptides were added in the cell culture medium 10 min prior addition of the transfection mix (FuGENE plus DNA). The empty vector was used to balance the transfected DNA concentration. NF-$\kappa$B-dependent luciferase assays were performed in

duplicate, and the data represent at least three independent experiments. Data show mean ± S.E.

*Site-directed Mutagenesis*—The 30 mutations introduced into the LRR domain of hNod1 were obtained individually by PCR, using standard procedures. Briefly, pairs of complementary oligonucleotides (see the list below) were designed to carry the mutation of interest. These oligonucleotides were used as primers for circular PCR, to amplify the whole pcI-hNod1 plasmid. Amplified plasmids were selected using the DpnI restriction enzyme. For each mutant, the HindIII-NotI domain spanning the LRR domain of hNod1 was then subcloned into a pcI-hNod1 vector that had not been subjected to PCR and had been fully sequenced previously. This subcloning step was performed to avoid possible mutations in the rest of the hNod1 cDNA sequence. Following subcloning, the whole HindIII-NotI region was fully sequenced (Millgen, France) to ensure that the mutation of interest was present and that no additional mutation was introduced by the PCR.

*Generation of Nod1 Isoforms Δ10, Δ10–11, and Δ10–12*—The three Nod1 constructs Δ10, Δ10–11, and Δ10–12 were generated by PCR according to standard methods. The oligonucleotides used are listed below. Briefly, couples of primers 1F/2R, 1F/2Rbis, 1F/2Rter, 3F/6R, 4F/6R, and 5F/6R were used to amplify regions of hNod1 by using full-length hNod1 expressing vector as a template, leading to the generation of PCR products A, B, C, D, E and F, respectively. PCR products A–F were excised from gel and purified, and A/D, B/E, and C/F were annealed and used together with primers 1F and 6R for a second round of PCR, therefore amplifying regions corresponding to constructs of interest D10, D10–11, and D10–12, respectively. Finally, PCR products were digested by using HindIII-NotI restriction enzymes, and the fragment obtained was used to exchange the HindII-NotI fragment from a new (non PCR-amplified) expression vector encoding for hNod1. Following subcloning, sequencing was performed (Millgen, France) to ensure that the right constructs were generated.

*Oligonucleotides Used for Site-directed Mutagenesis*—The following oligonucleotides were used: 1For GGGGCATCTGCGCCAACTCCC-TCAAGCTG and 1Rev CAGCTTGAGGGAGTTGGCGCAGATGC-CCC; 2For GCGCCAACTACCTCAGCCTGACCTACTGCAACGC-CTGC and 2Rev GCAGGCGTTGCAGTAGGTCAGGCTGAGGTA-GTTGGCGC; 3For GCCAACTACCTCAAGCTGGCCTACTGCAA-CGCCTGC and 3Rev GCAGGCGTTGCAGTAGGCCAGCTTGAG-GTAGTTGGC; 4For GCATCACTTCCCCAAGCGGCTGTCCCTA-GACCTAGACAAC and 4Rev GTTGTCTAGGTCTAGGGACAGC-CGCTTGGGGAAGTGATGC; 5For GGCTGGCCCTATCCCTAG-ACAACAACAATCTCAACGACTACGG and 5Rev CCGTAGTCGT-TGAGATTGTTGTTGTCTAGGGATAGGGCCAGCC; 6For GGC-TGGCCCTAGACCTATCCAACAACAATCTCAACGACTACGG and 6Rev CCGTAGTCGTTGAGATTGTTGTTGGATAGGTCTAG-GGCCAGCC; 7For GCTTCAGCCGCCTCACTGCTCTCAGACTC-AGCGTAAACC and 7Rev GGTTTACGCTGAGTCTGAGAGCAG-TGAGGCGGCTGAAGC; 8For GCCTCACTGTTCTCAGCCTCAG-CGTAAACCAGATCACTG and 8Rev CAGTGATCTGGTTTACGC-TGAGGCTGAGAACAGTGAGGC; 9For GCCGCCTCACTGTTC-TCAGACTCGCCGTAAACCAGATCACTG and 9Rev CAGTGATC-TGGTTTACGGCGAGTCTGAGAACAGTGAGGCGGC; 10For CA-AAAТTGTGACCTCTTTGGGTTTATACAACAACCAGATC and 10Rev GATCTGGTTGTTGTATAAACCCAAAGAGGTCACAAT-TTTG; 11For GTGACCTATTTGAGTTTATACAACAACCAGAT-CACCGATGTCGG and 11Rev CCGACATCGGTGATCTGGTTGT-TGTATAAACTCAAATAGGTCAC; 12For GTGACCTATTTGGG-TTTATCCAACAACCAGATCACCGATGTCGG and 12Rev CCGA-CATCGGTGATCTGGTTGTTGGATAAACCCAAATAGGTCAC;
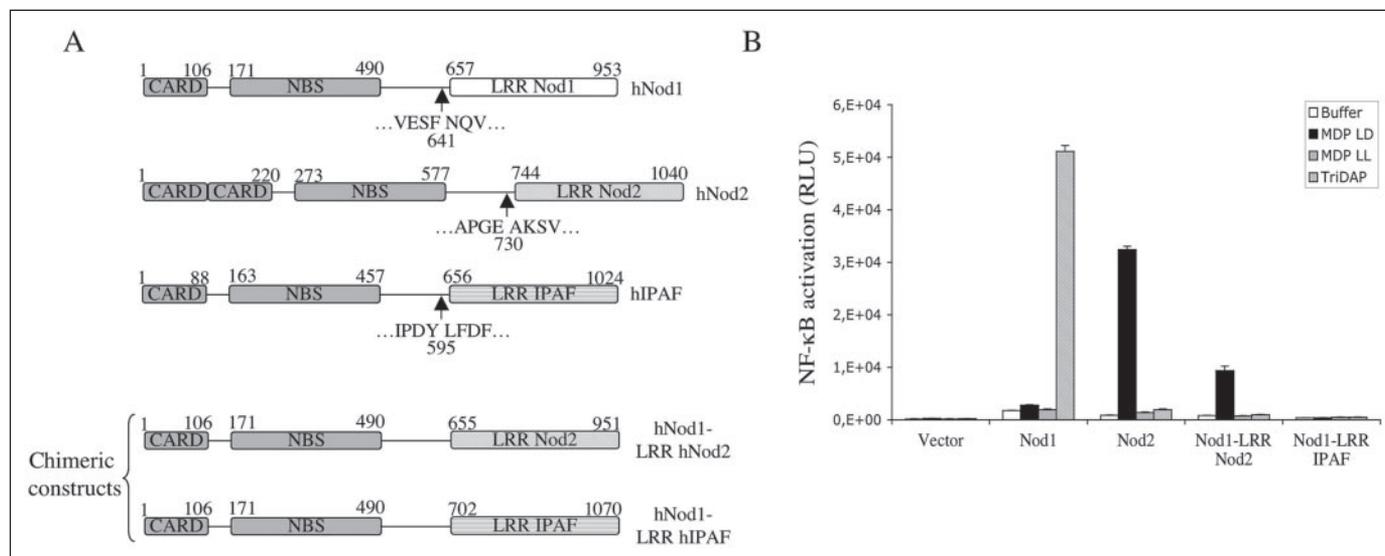
FIGURE 1. **The LRR domain is fully responsible for the sensing specificity of hNod1.** *A,* schematic representation of the domain organization of hNod1, hNod2, and hIPAF. The *upper numbers* represent the amino acid positions for the boundaries of each domain, plus the first and last amino acid of each protein. Below each representation is indicated the position selected for the domain swaps between hNod1 LRR and hNod2 LRR (creation of the chimeric molecule hNod1-LRR hNod2) or between hNod1 LRR and hIPAF LRR (creation of the chimeric molecule hNod1-LRR hIPAF). *B,* human HEK293 epithelial cells were co-transfected with several muramyl peptides (MDP LD, MDP LL, or Tri$_{DAP}$; all at 250 nM) in the presence of expression vectors for empty PcDNA$_3$ vector (*Vector*), hNod1 (*Nod1*), hNod2 (*Nod2*), or the chimeric molecules (*Nod1-LRR Nod2* or *Nod1-LRR IPAF*), and the activity of an NF-κB-driven luciferase reporter gene was measured. *RLU,* relative light units. Data show the mean ± S.E. of duplicate experiments. MDP LD is the natural product from bacterial cell wall. MDP LL is a biologically inactive enantiomer derivative of MDP.
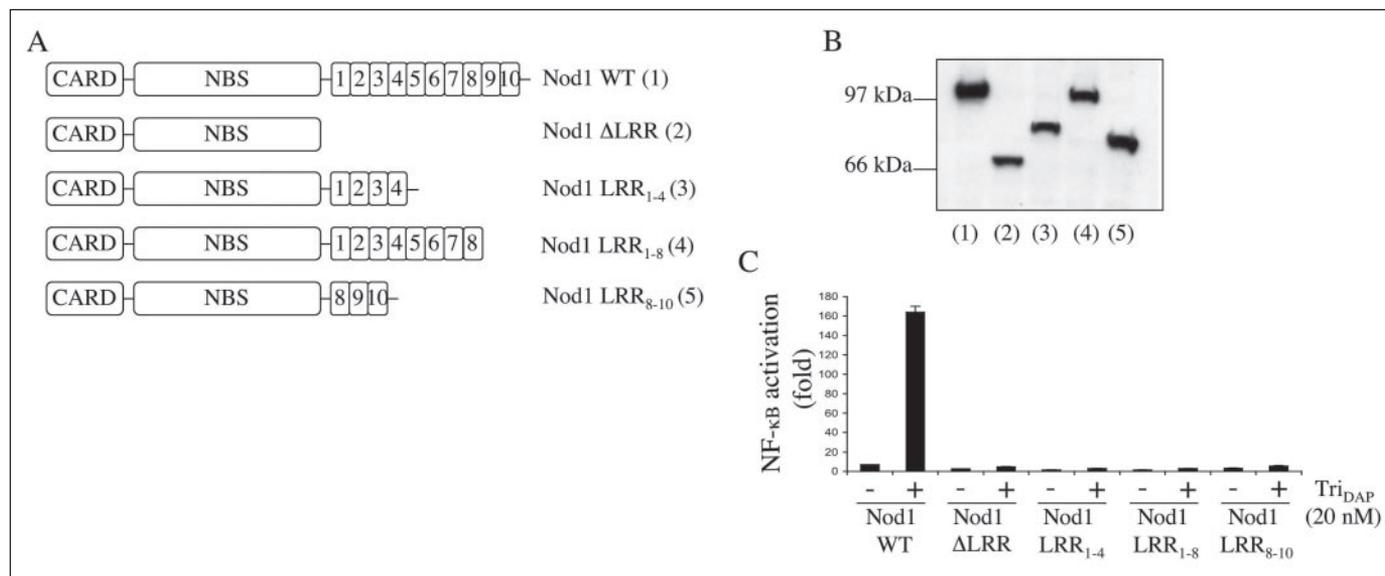


FIGURE 2. **Deletions in the LRR domain of hNod1 hamper sensing of Tri$_{DAP}$.** *A,* schematic representation of the domain organization of wild-type hNod1 (*1*) and of the four deletion constructs in the LRR domain (depicted as *2–5*). *B,* human HEK293 epithelial cells were transfected with 25 ng of expression vector for each of the five hNod1 constructs, and the expression of the five constructs was assessed by Western blot, using a polyclonal antibody against hNod1 recognizing epitopes in the CARD domain and the intermediary region between the NBS and the LRR domains. *C,* human HEK293 epithelial cells were co-transfected with expression vectors for hNod1 (*Nod1 WT*), *Nod1 ΔLRR*, *Nod1 LRR$_{1-4}$*, *Nod1 LRR$_{1-8}$*, or *Nod1 LRR$_{8-10}$*, in the presence or the absence of Tri$_{DAP}$ (as indicated on the figure; 20 nM), and the activity of a NF-κB-driven luciferase reporter gene was measured. Data show the mean ± S.E. of duplicates.

13For CCTGGATGAATGCAAAGGCCTCACGTCTCTTAAACT-GGGA and 13Rev TCCCAGTTTAAGAGACGTGAGGCCTTTGCA-TTCATCCAGG; 14For GAATGCAAAGGCCTCACGCATCTTAC-TCTGGGAAA and 14Rev TTTCCCAGAGTAAGATGCGTGAGGC-CTTTGCATTC; 15For GGCCTCACGCATCTTAAACTGTCAAA-AAACAAAATAACAAGTGAAGGAGGG and 15Rev CCCTCCTTC-ACTTGTTATTTTGTTTTTTGACAGTTTAAGATGCGTGAG-GCC; 16For GCAAATCAATCTCTTCGGTTGGGATGTGGGGCA-ATCAAGTTGGG and 16Rev CCCAACTTGATTGCCCCACATCC-CAACCGAAGAGATTGATTTGC; 17For GGTTTCGATGTGGGG-CAATCAAGTTGGGGATGAAGG and 17Rev CCTTCATCCCCAA-CTTGATTGCCCCACATCGAAACC; 18For GGTTGGGATGTCG-GGCAATCAAGTTGGGGATGAAGG and 18Rev CCTTCATCCCC-AACTTGATTGCCCGACATCCCAACC; 19For GCTTGACCGCC-CTGAGTCTTGCGTCCAACGG and 19Rev CCGTTGGACGCAAG-ACTCAGGGCGGTCAAGC; 20For GACCACCCTGGGTCTTGCG-TCCAACGGCATC and 20Rev GATGCCGTTGGACGCAAGACCC-AGGGTGGTC; 21For GCTTGACCACCCTGAGTCTTTCGTCCA-ACGG and 21Rev CCGTTGGACGAAAGACTCAGGGTGGTCA-AGC; 22For GCAGCAGAACACGTCTCTAGAAGCACTGTGGCT-GACCC and 22Rev GGGTCAGCCACAGTGCTTCTAGAGACGTG-TTCTGCTGC; 23For GTCTCTAGAAATACTGTCGCTGACCCA-
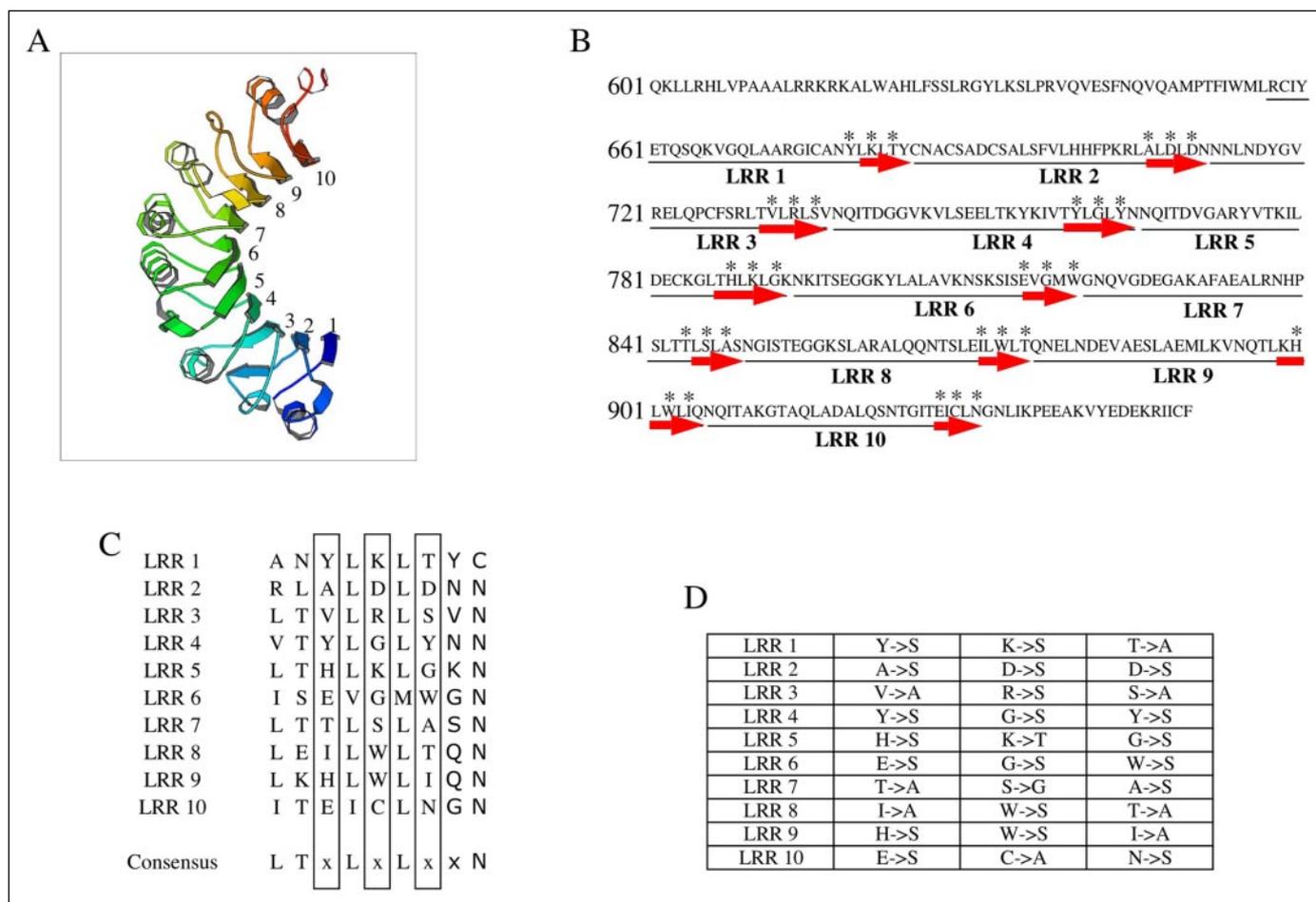
FIGURE 3. **Choice of the amino acids for site-directed mutagenesis in the LRR domain of hNod1.** *A,* homology model of hNod1 LRR. The *arrows* represent the β-strands from the C-terminal end of each repeat. *B,* amino acid sequence of hNod1 LRR domain showing the identity of the 30 mutations introduced (*asterisks*). The repeats are *underlined* and *numbered,* and the β-strands are represented by *red arrows. C,* alignment of the C-terminal extremity of the 10 repeats from the hNod1 LRR domain. All the amino acids selected for mutagenesis (3 per repeat) are highlighted by *black rectangles. D,* the nature of the amino acid change at each position is indicated. For each position, the replacement with either serine (*S*), alanine (*A*), threonine (*T*), or glycine (*G*) was designed in order to minimize the risk of altering the conformational organization of the LRR domain.

AAATGAACTC and 23Rev GAGTTCATTTTGGGTCAGCGACAG-TATTTCTAGAGAC; 24For GTCTCTAGAAATACTGTGGCTGG-CCCAAAATGAACTC and 24Rev GAGTTCATTTTGGGCCAGCC-ACAGTATTTCTAGAGAC; 25For GTCAACCAGACGTTAAAGT-CTTTATGGCTTATCCAGAATCAGATC and 25Rev GATCTGAT-TCTGGATAAGCCATAAAGACTTTAACGTCTGGTTGA; 26For GTCAACCAGACGTTAAAGCATTTATCGCTTATCCAGAA-TCAG and 26Rev CTGATTCTGGATAAGCGATAAATGCTTTAAC-GTCTGGTTGAC; 27For GTCAACCAGACGTTAAAGCATTTAT-GGCTTAGCCAGAATC and 27Rev GATTCTGGCTAAGCCATAA-ATGCTTTAACGTCTGGTTGAC; 28For GAGCAACACTGGCAT-AACATCGATTTGCCTAAATGGAAACCT and 28Rev CAGGTTT-CCATTTAGGCAAATCGATGTTATGCCAGTGTTGCTC; 29For GGCATAACAGAGATTTCCCTAAATGGAAACCTGATAAAAC-CAGAG and 29Rev CTCTGGTTTTATCAGGTTTCCATTTAGGG-AAATCTCTGTTATGCC; and 30For GGCATAACAGAGATTTGC-CTAAGTGGAAACCTGATAAAACC and 30Rev GGTTTTATCA-GGTTTCCACTTAGGCAAATCTCTGTTATGCC.

*Oligonucleotides Used for the Generation of Nod1 Constructs Δ10, Δ10–11, and Δ10–12*—The following oligonucleotides were used: 1F GCCTGCGGGGCTACCTGAAG; 2R GTGGAGATGCCGTTGGA-CGCAAGCCCAACCTCAGAGATTGATTTG; 3F GTTGGGCTTG-CGTCCAACGGCATCTCCAC; 6R CTAGTTGTGGTTTGTCCAA-ACTCATC; 4F GTTGGGCTGACCCAAAATGAACTCAACGATG;

2Rbis GTTGAGTTCATTTTGGGTCAGCCCAACCTCAGAGATT-GATTTG; 5F GTTGGGCTTATCCAGAATCAGATCACAGCT-AAG; and 2Rter CTTAGCTGTGATCTGATTCTGGATAAG-CCCAACCTCAGAGATTGATTTG.

## RESULTS

Early studies on Nod proteins Nod1 and Nod2 had demonstrated the key role of the LRR domain in achieving bacterial sensing (10, 19). However, it remains unclear whether the specificity for certain muropeptides (*i.e.* specific detection of MDP *versus* M-Tri$_{DAP}$) is carried exclusively by the LRR domain. To this end, we constructed chimeric molecules hNod1-LRRhNod2 and hNod1-LRRhIPAF in which the LRR domain of hNod1 was exchanged with the one for hNod2 and hIPAF, respectively (Fig. 1*A*). We observed that hNod1-LRRhNod2 could not detect Tri$_{DAP}$ but rather MDP (Fig. 1*B*), thereby showing that the LRR domain is responsible for the specific detection of muropeptides by Nod molecules. As a negative control, swapping the LRR domains of Nod1 and IPAF (a molecule closely related to Nod1 and Nod2) resulted in a molecule (hNod1-LRRhIPAF) unable to detect both Tri$_{DAP}$ and MDP (Fig. 1*B*), although expressions of hNod1-LRRhNod2 and hNod1-LRRhIPAF were comparable (data not shown). It must be noted that hNod1-LRRhNod2, as does Nod2, detected specifically MDP LD, but not the inactive enantiomer MDP LL (Fig. 1*B*). This illustrates the fact that LRR
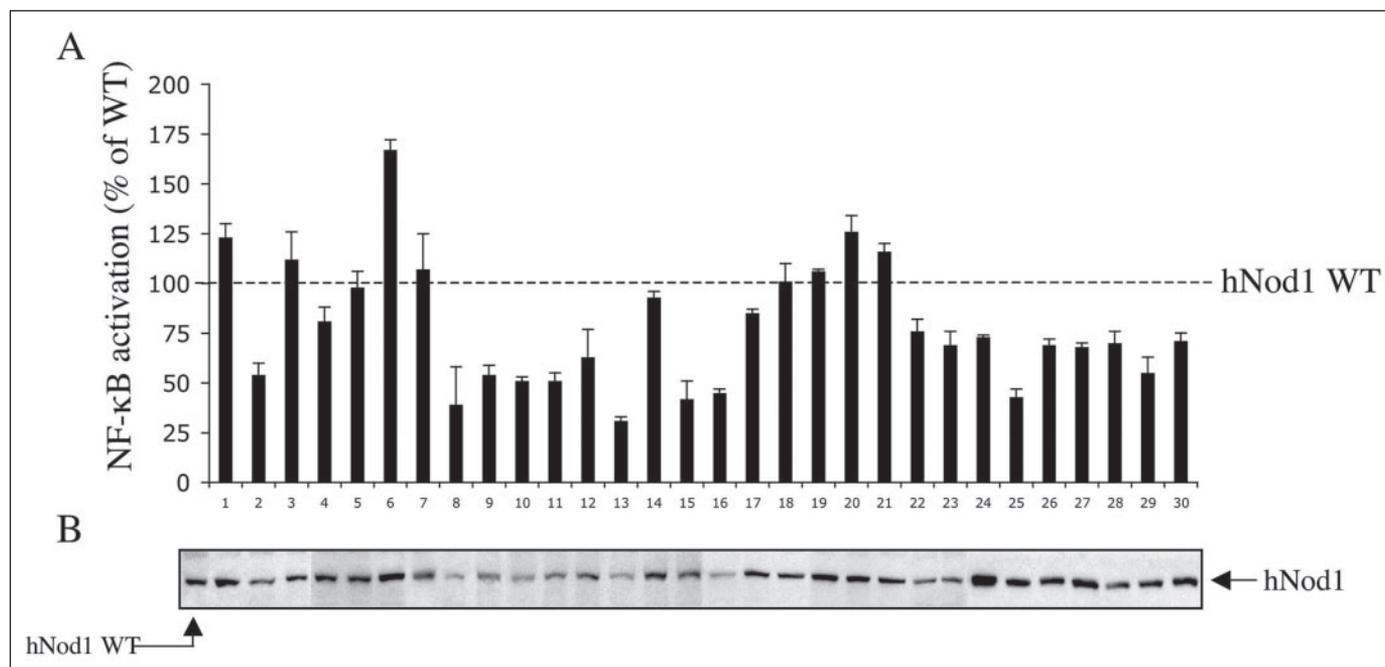
FIGURE 4. **Autoactivation of the 30 mutants in the LRR domain of hNod1.** *A,* human HEK293 epithelial cells were transfected with 25 ng of expression vectors encoding for hNod1 mutations 1–30, according to numbering from the N terminus to the C terminus of the LRR domain. The activity of an NF-$\kappa$B-driven luciferase reporter gene induced by the simple overexpression of each mutant in HEK293 cells was measured. For each mutant, the results obtained are from three independent experiments done in duplicate; the six values of NF-$\kappa$B activation obtained were then pooled and reported to the level of activation by wild-type (*WT*) hNod1. *B,* cellular extracts from HEK293 cells analyzed in *A* were collected (six independent points per mutant were pooled) and analyzed for expression of the mutant forms of hNod1 by Western blot, using a polyclonal antibody against hNod1. The relative expression level of each mutant can be compared with the one of wild-type Nod1 presented on the *1st lane* of the Western blot. Note that the differences in autoactivation by overexpression of the mutants (seen in *A*) strongly correlate with the relative expression of each mutant (seen in *B*). This suggests that the mutations are likely to affect the expression/stability of hNod1 rather than the intrinsic ability of the molecule to activate the NF-$\kappa$B pathway.

domains carry the global specificity for muropeptide detection, even at the stereoisomeric level.

In an attempt to narrow down the region responsible for $Tri_{DAP}$ sensing in hNod1 LRR, several deletion mutants were generated (Fig. 2, *A* and *B*). However, this strategy was inappropriate because none of the mutants could retain any sensing of $Tri_{DAP}$ (Fig. 2*C*), strongly suggesting that the structural integrity of the LRR domain is required to achieve full muropeptide detection. Next, an approach based on single amino acid mutagenesis was chosen. The LRR domain of hNod1 contains 10 repeats and is expected to fold into the right-handed, curved solenoid structure characteristic of these proteins (Fig. 3*A*). In most LRR domains, the long $\beta$-sheet forming the inner concave face is usually involved in protein-protein interactions (27). Therefore, we selected three positions at the center of the $\beta$-strand from each repeat, whose side chains are predicted to be accessible for ligand interactions and generated 30 mutants in hNod1 LRR (Fig. 3*B*). By the strategy used, all mutations could be aligned to corresponding positions within each repeat (Fig. 3*C*). In order to minimize the risk of generating mutant molecules that would be unstable or misfolded because of the amino acid exchange, the substitutions chosen were variable depending on the nature of the amino acid to replace (Fig. 3*D*). All these mutants were expressed and retained their basal capacity to activate the NF-$\kappa$B pathway when overexpressed (Fig. 4*A*). It must be noted that most of the differences in NF-$\kappa$B activation between the 30 mutants correlated with expression levels, as determined by Western blotting (Fig. 4*B*). Therefore, we concluded from these experiments that none of the mutants displayed any drastic artifactual loss of function because of defects of expression or stability. Next, each mutant was compared with the wild-type form of hNod1 for its capacity to detect $Tri_{DAP}$ (Fig. 5*A*). We observed that mutations in the fifth and sixth repeats (mutants 13–18), as well as mutation 23 (W874S) in repeat 8, dramatically affected sens-

ing, reducing $Tri_{DAP}$ detection by more than 80%. Mapping the effect of these mutants into the concave surface of hNod1 LRR revealed that the amino acid residues critically affecting $Tri_{DAP}$ sensing define a contiguous patch toward the C-terminal end of the middle $\beta$-strands (Fig. 5*B*, *left*), which closely matches the pattern of strictly conserved residues in available Nod1 sequences from different species (Fig. 5*B*, *right*).

We have demonstrated recently that human and murine forms of Nod1 do not detect the same muropeptide from bacterial peptidoglycan (28). Indeed, although the human form of Nod1 detected a tripeptide-containing muropeptide (MurNAc-$Tri_{DAP}$ or $Tri_{DAP}$), its murine ortholog needs a tetrapeptide structure for efficient sensing (MurNAc-$Tetra_{DAP}$ or $Tetra_{DAP}$). Therefore, the synthetic compound, FK156 (lactoyl-$Tetra_{DAP}$), represents an efficient agonist for mNod1 (28). We thus aimed to investigate whether the distinct agonist specificities of hNod1 and mNod1 also match the sensing pocket identified above. Taking advantage of our observation that a high concentration of FK156 (250 nM) can potentiate hNod1-dependent NF-$\kappa$B activation $\sim$7-fold (28), we screened the collection of 30 point mutants of hNod1 to investigate whether any of these would display better detection of FK156. Although for most of the mutants the level of residual activation by FK156 remained close to or below the detection limit of the test, two particular mutants (16 and 19) were activated significantly better than wild-type hNod1 (Fig. 6*A*).Most interestingly, mutant 16 is found at the periphery of the contiguous patch defined above (see Fig. 5*B*) and is the only amino acid of this pocket that is not conserved between hNod1 and mNod1. Both mutation 16 (E816S) and the mutation that directly mimics the amino acid difference between hNod1 and mNod1 (E816D) improved equally well the sensing of FK156 by hNod1 (data not shown). Mutation 19 (T844A) affects an amino acid position that, although conserved between hNod1 and mNod1, is spatially adjacent to Glu-816 and is surrounded by additional nonconserved residues between hNod1 and
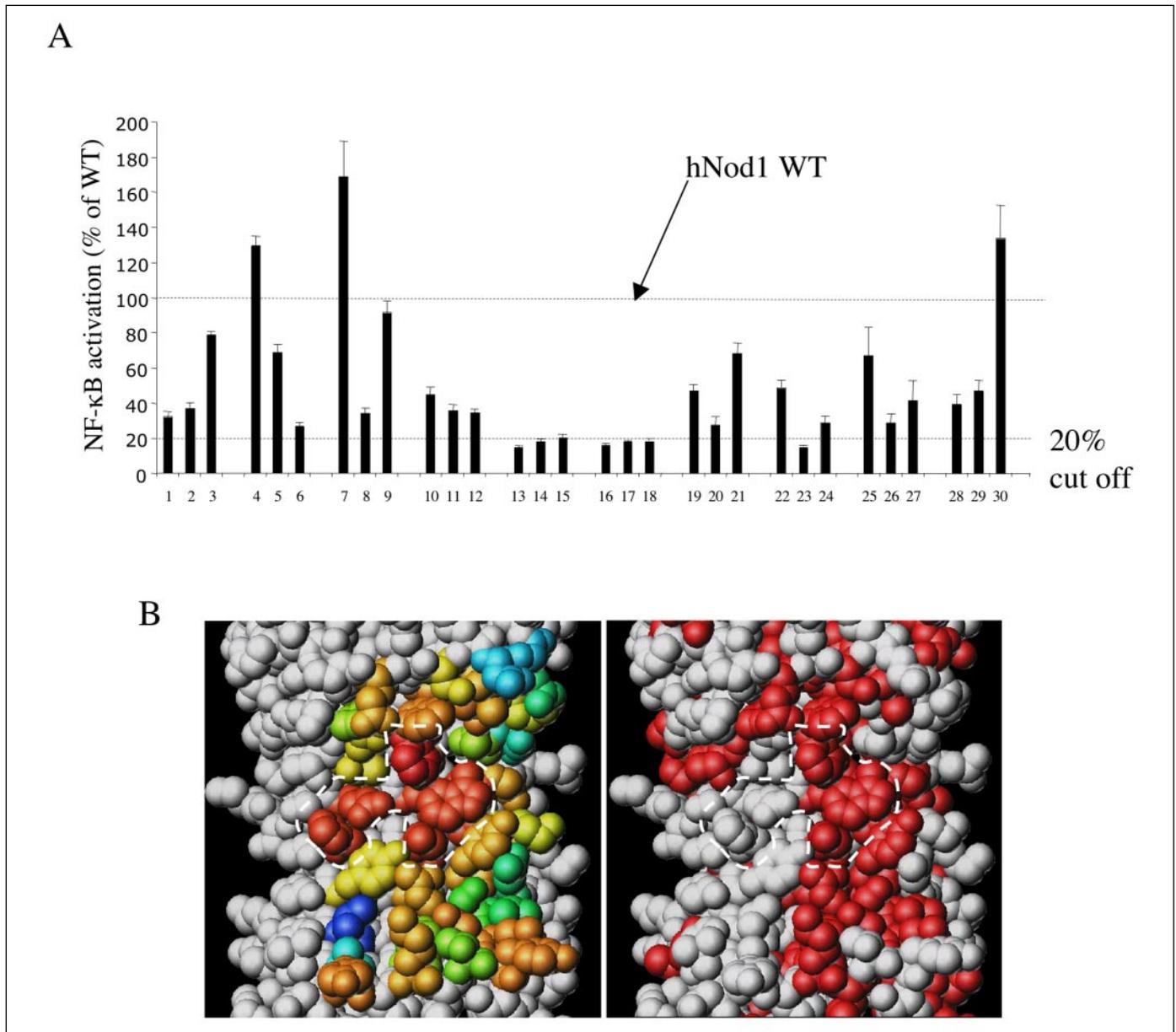
FIGURE 5. **Identification of the region responsible for specific muramyl peptide detection within hNod1 LRR domain.** *A,* human HEK293 epithelial cells were transfected with each mutant (numbered from 1 to 30) in the presence or absence of $Tri_{DAP}$ (20 nM) as an agonist. For each mutant, the fold of NF-κB activation resulting from activation by $Tri_{DAP}$ was reported as a percentage to the one of wild-type hNod1 (*dashed line* at 100%). Data show the mean ± S.E. of duplicates. *B,* view of the exposed residues in the concave face of the LRR domain (same view as in Fig. 3*A*, rotated 90° along the vertical axis). The *left diagram* displays the relative importance of each mutated amino acid in the detection of $Tri_{DAP}$. The color code illustrates the results obtained in *A*: from *blue* to *red*, increasing importance of each position for $Tri_{DAP}$ sensing. The *right diagram* shows in *red* the amino acids that are 100% identical in Nod1 protein sequences from human, mouse, rat, fish, and chicken (the five animal species for which a Nod1 ortholog has currently been identified). On both diagrams, a *dashed line* illustrates the topological area critical for $Tri_{DAP}$ sensing.

mNod1 (Fig. 6*B*, *right*). Together, these results strongly suggested that we have mapped the region responsible for $Tri_{DAP}$ sensing in hNod1 and identified a particular site (around amino acids 816 and 844) critical for the specific detection of DAP-containing tetrapeptide *versus* tripeptide muropeptides.

Several isoforms of Nod1 have been characterized recently as a result of alternative splicing, thus giving rise to Nod1 molecules lacking repeats 7, 7–8, or 7–8-9 (24). Two recent studies have suggested that the relative expression of Nod1 splice variants could correlate with the onset of asthma and inflammatory bowel disease (22, 24). These isoforms differ at the level of the LRR domain, and the splicing site is located at the junction between exons 10 and 11, in the heart of the $Tri_{DAP}$ sensing pocket that we have identified (in the next vicinity to

amino acids corresponding to mutations 16, 17, and 18). Therefore, we aimed to investigate how these isoforms detect $Tri_{DAP}$. We generated by PCR the three constructs, Nod1Δ10, Nod1Δ10–11, and Nod1Δ10–12, corresponding exactly to the alternative splice variants of Nod1 (Fig. 7*A*). These molecules were expressed and displayed the expected molecular weight as observed by Western blotting (Fig. 7*B*). In addition, the three splicing variants were able to activate the NF-κB pathway when overexpressed (Fig. 7*C*), thus showing that these molecules do not display gross defects in transducing downstream signals. However, none of the three splicing isoforms were able to activate the NF-κB pathway in response to $Tri_{DAP}$ stimulation, even at high concentrations of the agonist. Indeed, 250 nM of $Tri_{DAP}$ is a concentration ~100 times higher than the minimal concentration activating full-length Nod1

(data not shown). Therefore, the three naturally occurring splicing variants of Nod1 were unable to induce NF-κB activation following stimulation with the peptidoglycan agonist. This correlates with our characterization of the critical residues involved in Tri$_{DAP}$ detection; the splicing site at residue 819 (see Fig. 7A) is located in the heart of the sensing patch defined above. Therefore, it is likely that alternative splicing occurring within Nod1 LRR domain may represent a physiological means to drop off Nod1 signaling.

## DISCUSSION

In this study, an analysis of the putative ligand-sensing domain of Nod1 was carried out in order to determine key regions necessary for ligand recognition. We took a systematic approach of site-directed mutagenesis focusing on the residues that lie within the concave portion of the leucine-rich repeat domain and are predicted to be accessible for ligand binding. Assuming a solenoid-like structure for the LRR domain of Nod1 similar to that of other homologous LRR proteins, conservative amino acid substitutions were thus carried out on three equivalent positions of each putative β-strand. By using this strategy, a peptidoglycan detection patch was identified within repeats 5–7, a region that is highly conserved in the Nod1 sequence from different species. Moreover, we were able to map what are likely to be the key residues involved in differential ligand sensing of mouse and human forms of Nod1. Finally, with this knowledge, the function of different naturally occurring isoforms of Nod1 that lack central LRRs within the interaction domain could then be postulated. Our speculation is that in certain disease states or perhaps in normal physiological conditions, expression of these isoforms would down-regulate Nod1 function thereby favoring the development of disease in some cases, although in others, this function may form an important regulatory loop to help terminate signals emanating from Nod molecules.

To date, studies on receptor-ligand interactions of PRMs and their microbial motif elicitors have been hampered by technical problems, and only in a few instances have studies been able to show direct interactions. Recently, Toll in *Drosophila* was shown to interact directly with its ligand, spaztle (29). Similarly, TLR5 has been shown to interact with its protein ligand flagellin (30). In the case of some PRMs, like TLR4 for example, demonstration of a direct interaction with the agonist, lipopolysaccharide, has not been possible because of the fact that co-receptors are required for this interaction. For NLRs, there are no data at the moment that implicate direct interaction between Nod1 or Nod2 and their specific muropeptide ligands. In the case of Nod1, the insolubility of the protein in overexpression systems and the uncertainty as to whether proper folding occurs *in vitro* has hampered any possibilities to test whether or not there is a direct interaction with Tri$_{DAP}$.[4] Therefore, as an alternative approach, we embarked on a study to identify regions within the Nod1 molecule that are necessary for sensing and not necessarily for direct interaction because we cannot rule out that cofactor molecules could be involved. By using chimeric molecules swapping LRR domains between Nod1 and Nod2 and Nod1 and Ipaf, it was shown conclusively that the LRR domain carries the sensing specificity of Nod proteins toward their muropeptide agonist. Furthermore, a deletion and loss of function approach demonstrated that deletions within the LRR domain are likely to affect the tertiary structure of the molecule, thus ruling out the validity of this approach to map the interaction domain.

By using a random mutagenesis approach, Nuñez and co-authors (31) mapped a number of sites both in the convex and concave regions
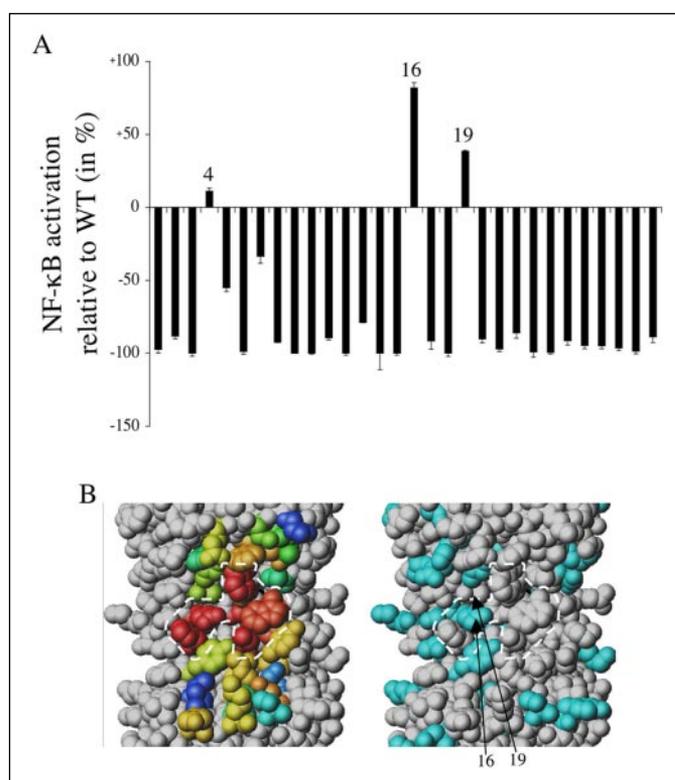
FIGURE 6. **Amino acids involved in defining the specificity of hNod1 and mNod1 for muropeptides also located in the vicinity of the Nod1 sensing patch.** *A,* human HEK293 epithelial cells were transfected with each mutant (numbered from 1 to 30) in the presence or absence of FK156 (250 nM) as an agonist. For each mutant, the fold of NF-κB activation resulting from activation by FK156 was reported as a percentage of modification to the one of wild-type hNod1 (0% represents sensing of FK156 equivalent to the one of hNod1). Data show the mean ± S.E. of duplicates. *B,* view of the exposed residues in the concave face of the LRR domain (same view as in Fig. 3A, rotated 90° along the vertical axis). The *left diagram* is identical to the one in Fig. 5B, *left.* The *right diagram* shows in *cyan* the amino acids differing in the human and mouse sequences of Nod1. On both diagrams, a *dashed line* illustrates the topological area critical for Tri$_{DAP}$ sensing. The amino acids corresponding to mutations 16 (E816D) and 19 (T844A) are indicated by *arrows.*

of Nod2 that appear to be important for the activity of the molecule (31). Many of these sites are located in the middle and C-terminal end of the concave portion of the LRR, although it is unclear whether some of the mutations also affect the basal activity of the molecule because of the random nature of the amino acid substitutions. Nevertheless, it is interesting to note that the most frequent mutation in *Nod2* (Nod2 1007fs mutation), associated with Crohn disease in humans, also maps to the C-terminal portion of the LRR. This mutation results in a loss of sensing of the MDP agonist by Nod2 (7, 9). Taken together, these findings suggest that in both Nod1 and Nod2, the central to C-terminal regions of the LRR appear to be a "hot spot" in terms of muropeptide sensing.

Within this putative binding patch of the LRR of Nod1, we could also identify key residues that contribute to the differential agonist sensing between human and murine Nod1. Our recent data show (28) that human and murine forms of Nod1 strictly sense DAP-containing muropeptides, but murine Nod1 prefers muropeptides with four rather than three amino acids within the peptide chain. Human and murine forms of Nod1 therefore present very little overlap in the muropeptide agonist that they recognize, and our results demonstrate that this can be attributed, at least in part, to differences in a few amino acids within the LRR domain of Nod1.

Two recent studies have implicated polymorphisms in the gene encoding Nod1 in the development of asthma and inflammatory bowel disease. The polymorphisms lie within intron nine, and both studies
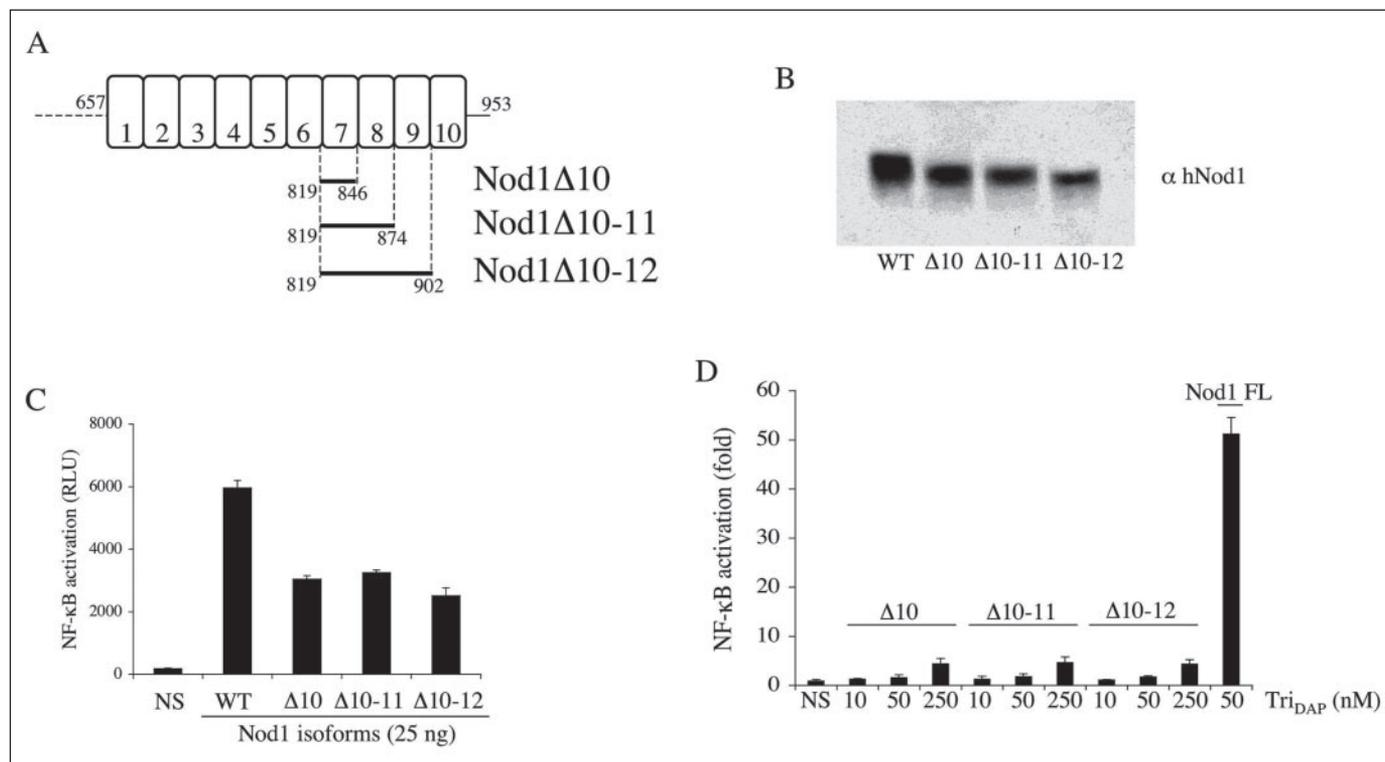
FIGURE 7. **Nod1 splicing variants fail to detect Tri$_{DAP}$.** *A,* schematic representation of the position where alternative splicing occurs within the Nod1 LRR domain, giving rise to three spliced isoforms, *Nod1Δ10, Nod1Δ10–11,* and *Nod1Δ10–12,* lacking exons 10, 10–11, and 10–11-12, respectively. Note that exons 10–12 precisely match repeats 7–9 within Nod1 LRR (see also Fig. 3B for the precise position of each repeat along Nod1 primary sequence). *B,* expression profile of Nod1, Nod1Δ10, Nod1Δ10–11, and Nod1Δ10–12 as determined by Western blotting, using a polyclonal antibody raised against Nod1. For this purpose, HEK293 cells have been transfected with 25 ng of expression vector (plus 75 ng of IgK-luc reporter construct; see below) encoding Nod1 full-length or its spliced isoforms. *WT,* wild type. *C,* cellular extracts that were used for Western blotting (see *B*) were tested in parallel for NF-κB activation as described in legend for Fig. 4. Data show the mean ± S.E. of duplicate experiments. *D,* human HEK293 epithelial cells were co-transfected with expression vectors for Nod1Δ10, Nod1Δ10–11, and Nod1Δ10–12, in the presence of increasing concentrations of Tri$_{DAP}$ (as indicated on the figure; 10, 50, or 250 nM), and the activity of a NF-κB-driven luciferase reporter gene was measured. As a positive control, activation of Nod1 full-length (Nod1 FL) by 50 nM Tri$_{DAP}$ was performed. Data are presented as fold activation over NF-κB activation induced by each individual construct. Data show the mean ± S.E. of duplicates. *NS,* not stimulated.

suggest that this mutation may contribute to differences in expression levels of naturally occurring splice variants of Nod1. In normal tissue, isoforms of Nod1 are readily detected that lack either the 7th, 7th to 8th, or 7th to 9th repeats within the LRR domain. According to our studies, these isoforms should have the recognition site at least partially interrupted. Therefore, our goal was to examine these isoforms for their function in terms of muropeptide agonist sensing in comparison with full-length Nod1. Although they maintained the ability to activate the NF-κB pathway in overexpression studies, none of the truncated isoforms were able to sense Tri$_{DAP}$ compared with the activity of full-length Nod1. These findings suggest that at physiological levels, Nod1 splicing variants may contribute to shutting down the NF-κB pathway triggered by the full-length molecule. In that regard, these isoforms may be up-regulated by inflammatory stimuli in order to dampen Nod-dependent signals. In terms of disease, the expression of these isoforms may be altered during different disease states, as has been suggested in asthma or inflammatory bowel disease (22, 24). In the future, it will be interesting to examine the expression of these isoforms in different disease states and how they then may impact on the development of disease.

Regulation of the biological activity of NLR family members through alternative splicing occurring in the LRR domain might represent a common theme. Indeed, splicing variants within Monarch-1/PYPAF7/NALP12 LRR domain are strikingly reminiscent of those in Nod1 (32). Similarly, CIAS1/PYPAF1/NALP3/Cryopyrin is expressed as several isoforms, generated by alternative splicing in the LRR domain (33). For most of the other members of the NLR family, this information is not yet available, but one can anticipate that similar findings will also hold true for other NLRs. In the case of *Nod2*, alternative splicing has not been investigated so far, but in view of our results and of the position of the most frequent mutation of Nod2 associated in Crohn disease (Nod2fs, mutation in the C-terminal end of the LRR domain), it might be worthwhile investigating this question in further detail.

In summary, our findings have defined a region within the LRR of Nod1 that appears to be critical for the sensing of Tri$_{DAP}$ by this molecule. Within this region, there are key amino acid residues that contribute to the differential agonist sensing between human and murine Nod1. As it stands, much of these data support the idea that the interaction of Nod1 with its peptidoglycan agonist/ligand is direct, unlike the situation that is often the case in other PRMs, including plant NBS-LRR proteins, where cofactors are implicated in sensing (34). It is hoped that future studies will address this issue. Furthermore, our definition of a critical sensing region within the LRR of Nod1 led us to examine naturally occurring spliced variants of Nod1 that lack LRRs C-terminal to this domain. These isoforms display a clear defect in muropeptide sensing. Because different disease states may favor differential expression of these isoforms, the next goal will be to try to understand the mechanisms by which alteration of Nod1 sensing by these isoforms may contribute to the development of disease.

## REFERENCES

1. Girardin, S. E., and Philpott, D. J. (2004) *Eur. J. Immunol.* **34,** 1777–1782
2. Steiner, H. (2004) *Immunol. Rev.* **198,** 83–96
3. Chamaillard, M., Inohara, N., and Nunez, G. (2004) *Trends Microbiol.* **12,** 529–532
4. Ting, J. P., and Davis, B. K. (2005) *Annu. Rev. Immunol.* **23,** 387–414
5. Chamaillard, M., Girardin, S. E., Viala, J., and Philpott, D. J. (2003) *Cell. Microbiol.* **5,** 581–592
6. Chamaillard, M., Hashimoto, M., Horie, Y., Masumoto, J., Qiu, S., Saab, L., Ogura, Y., Kawasaki, A., Fukase, K., Kusumoto, S., Valvano, M. A., Foster, S. J., Mak, T. W., Nunez, G., and Inohara, N. (2003) *Nat. Immun.* **4,** 702–707
7. Inohara, N., Ogura, Y., Fontalba, A., Gutierrez, O., Pons, F., Crespo, J., Fukase, K., Inamura, S., Kusumoto, S., Hashimoto, M., Foster, S. J., Moran, A. P., Fernandez-Luna, J. L., and Nunez, G. (2003) *J. Biol. Chem.* **278,** 5509–5512
8. Girardin, S. E., Travassos, L. H., Herve, M., Blanot, D., Boneca, I. G., Philpott, D. J., Sansonetti, P. J., and Mengin-Lecreulx, D. (2003) *J. Biol. Chem.* **278,** 41702–41708
9. Girardin, S. E., Boneca, I. G., Viala, J., Chamaillard, M., Labigne, A., Thomas, G., Philpott, D. J., and Sansonetti, P. J. (2003) *J. Biol. Chem.* **278,** 8869–8872
10. Girardin, S. E., Boneca, I. G., Carneiro, L. A., Antignac, A., Jehanno, M., Viala, J., Tedin, K., Taha, M. K., Labigne, A., Zahringer, U., Coyle, A. J., DiStefano, P. S., Bertin, J., Sansonetti, P. J., and Philpott, D. J. (2003) *Science* **300,** 1584–1587
11. Opitz, B., Forster, S., Hocke, A. C., Maass, M., Schmeck, B., Hippenstiel, S., Suttorp, N., and Krull, M. (2005) *Circ. Res.* **96,** 319–326
12. Opitz, B., Puschel, A., Schmeck, B., Hocke, A. C., Rosseau, S., Hammerschmidt, S., Schumann, R. R., Suttorp, N., and Hippenstiel, S. (2004) *J. Biol. Chem.* **279,** 36426–36432
13. Viala, J., Chaput, C., Boneca, I. G., Cardona, A., Girardin, S. E., Moran, A. P., Athman, R., Memet, S., Huerre, M. R., Coyle, A. J., DiStefano, P. S., Sansonetti, P. J., Labigne, A., Bertin, J., Philpott, D. J., and Ferrero, R. L. (2004) *Nat. Immun.* **5,** 1166–1174
14. Kim, J. G., Lee, S. J., and Kagnoff, M. F. (2004) *Infect. Immun.* **72,** 1487–1495
15. Girardin, S. E., Tournebize, R., Mavris, M., Page, A. L., Li, X., Stark, G. R., Bertin, J., DiStefano, P. S., Yaniv, M., Sansonetti, P. J., and Philpott, D. J. (2001) *EMBO Rep.* **2,** 736–742
16. Kobayashi, K. S., Chamaillard, M., Ogura, Y., Henegariu, O., Inohara, N., Nunez, G., and Flavell, R. A. (2005) *Science* **307,** 731–734
17. Travassos, L. H., Carneiro, L. A., Girardin, S. E., Boneca, I. G., Lemos, R., Bozza, M. T., Domingues, R. C., Coyle, A. J., Bertin, J., Philpott, D. J., and Plotkowski, M. C. (2005) *J. Biol. Chem.* **280,** 36714–36718
18. Hugot, J. P., Chamaillard, M., Zouali, H., Lesage, S., Cezard, J. P., Belaiche, J., Almer, S., Tysk, C., O'Morain, C. A., Gassull, M., Binder, V., Finkel, Y., Cortot, A., Modigliani, R., Laurent-Puig, P., Gower-Rousseau, C., Macry, J., Colombel, J. F., Sahbatou, M., and Thomas, G. (2001) *Nature* **411,** 599–603
19. Ogura, Y., Bonen, D. K., Inohara, N., Nicolae, D. L., Chen, F. F., Ramos, R., Britton, H., Moran, T., Karaliuskas, R., Duerr, R. H., Achkar, J. P., Brant, S. R., Bayless, T. M., Kirschner, B. S., Hanauer, S. B., Nunez, G., and Cho, J. H. (2001) *Nature* **411,** 603–606
20. Miceli-Richard, C., Lesage, S., Rybojad, M., Prieur, A. M., Manouvrier-Hanu, S., Hafner, R., Chamaillard, M., Zouali, H., Thomas, G., and Hugot, J. P. (2001) *Nat. Genet.* **29,** 19–20
21. Rose, C. D., Doyle, T. M., McIlvain-Simpson, G., Coffman, J. E., Rosenbaum, J. T., Davey, M. P., and Martin, T. M. (2005) *J. Rheumatol.* **32,** 373–375
22. McGovern, D. P., Hysi, P., Ahmad, T., van Heel, D. A., Moffatt, M. F., Carey, A., Cookson, W. O., and Jewell, D. P. (2005) *Hum. Mol. Genet.* **14,** 1245–1250
23. Weidinger, S., Klopp, N., Rummler, L., Wagenpfeil, S., Novak, N., Baurecht, H. J., Groer, W., Darsow, U., Heinrich, J., Gauger, A., Schafer, T., Jakob, T., Behrendt, H., Wichmann, H. E., Ring, J., and Illig, T. (2005) *J. Allergy Clin. Immunol.* **116,** 177–184
24. Hysi, P., Kabesch, M., Moffatt, M. F., Schedel, M., Carr, D., Zhang, Y., Boardman, B., von Mutius, E., Weiland, S. K., Leupold, W., Fritzsch, C., Klopp, N., Musk, A. W., James, A., Nunez, G., Inohara, N., and Cookson, W. O. (2005) *Hum. Mol. Genet.* **14,** 935–941
25. Choe, J., Kelker, M. S., and Wilson, I. A. (2005) *Science* **309,** 581–585
26. Inohara, N., Ogura, Y., Chen, F. F., Muto, A., and Nunez, G. (2001) *J. Biol. Chem.* **276,** 2551–2554
27. Schubert, W. D., Urbanke, C., Ziehm, T., Beier, V., Machner, M. P., Domann, E., Wehland, J., Chakraborty, T., and Heinz, D. W. (2002) *Cell* **111,** 825–836
28. Magalhaes, J. G., Philpott, D. J., Nahori, M.-A., Jéhanno, M., Fritz, J., Bourhis, L. L., Viala, J., Hugot, J.-P., Giovannini, M., Bertin, J., Lepoivre, M., Mengin-Lecreulx, D., Sansonetti, P. J., and Girardin, S. E. (October 7, 2005) *EMBO Rep.* 10.1038/sj.embor.7400552
29. Weber, A. N., Tauszig-Delamasure, S., Hoffmann, J. A., Lelievre, E., Gascan, H., Ray, K. P., Morse, M. A., Imler, J. L., and Gay, N. J. (2003) *Nat. Immun.* **4,** 794–800
30. Smith, K. D., Andersen-Nissen, E., Hayashi, F., Strobe, K., Bergman, M. A., Barrett, S. L., Cookson, B. T., and Aderem, A. (2003) *Nat. Immun.* **4,** 1247–1253
31. Tanabe, T., Chamaillard, M., Ogura, Y., Zhu, L., Qiu, S., Masumoto, J., Ghosh, P., Moran, A., Predergast, M. M., Tromp, G., Williams, C. J., Inohara, N., and Nunez, G. (2004) *EMBO J.* **23,** 1587–1597
32. Ting, J. P., and Williams, K. L. (2005) *Clin. Immunol.* (*Orlando*) **115,** 33–37
33. O'Connor, W., Jr., Harton, J. A., Zhu, X., Linhoff, M. W., and Ting, J. P. (2003) *J. Immunol.* **171,** 6329–6333
34. Belkhadir, Y., Subramaniam, R., and Dangl, J. L. (2004) *Curr. Opin. Plant Biol.* **7,** 391–399